

Magnetic-Field-Induced Laser Cooling below the Doppler Limit

B. Sheehy, S-Q. Shang, P. van der Straten, S. Hatamian,^(a) and H. Metcalf
Physics Department, State University of New York, Stony Brook, New York 11794

(Received 1 November 1989)

We report a new cooling scheme used to actively collimate an atomic beam of ^{85}Rb with one-dimensional optical molasses. The atoms' transverse velocity is damped by a standing wave of circularly polarized light in a magnetic field of $\sim 20 \mu\text{T}$ to 2 cm/s (rms), well below the Doppler velocity $v_D = (7\hbar\gamma/20M)^{1/2} \sim 10$ cm/s for one-dimensional optical molasses. The minimum measured velocity is limited only by the experimental geometry. We have developed a model in which the mixing by the field and optical pumping combine to form a cycle that cools below the Doppler limit, in agreement with our measurements.

PACS numbers: 32.80.Pj, 42.50.Vk

The early ideas of cooling atoms with laser light^{1,2} have been followed by increasing activity in both theory and experiment.³⁻¹¹ Theoretically the lowest obtainable temperature for optical cooling of two-level atoms is the Doppler temperature¹² $T_D = \hbar\gamma/2k_B$ ($\sim 140 \mu\text{K}$ for Rb), where γ is the natural linewidth ($\sim 2\pi \times 6$ MHz for Rb). Although the first experiments⁵ were consistent with this limit, later experiments yielded much lower temperatures.^{6,9,10} Recent theories^{13,14} explain these lower temperatures. Their important common feature is that real atoms have multiple magnetic sublevels whose different responses to the light result in forces much larger than the Doppler force.

One of the physical ideas of these models is the different light shifts (ac Stark shift) of the ground-state magnetic sublevels caused by the different couplings with the light. Light tuned below resonance causes a negative light shift for the ground-state sublevels and optically pumps atoms to the lowest sublevel. Atoms absorb light with lower frequency than they fluoresce, thus losing energy. To sustain the cooling process, atoms must be redistributed among the sublevels when the light shifts are smaller or reversed, and this arises from the polarization changes seen by a moving atom in a light field with polarization gradients.^{13,14} Reference 13 analyzes specific cases and obtains final temperatures much lower than T_D . Although the experiments used different setups,^{6,9,10} it is generally agreed that polarization gradients cause the observed sub-Doppler temperatures.

We have discovered a new cooling process that uses a standing wave with uniform polarization and a transverse magnetic field, whose role is to mix the differently light-shifted atomic ground-state sublevels.¹⁵ We have used this process for optical collimation of a Rb atomic beam to well below the transverse velocity $v_D = (7\hbar\gamma/20M)^{1/2} \cong 10$ cm/s expected for two-level atoms in a one-dimensional optical molasses.¹⁶ When the laser is tuned below resonance, atoms traveling across the standing wave will be optically pumped to the lowest-energy sublevel near an antinode, and redistributed among the

higher sublevels near a node by Larmor precession. Travel across the next antinode repeats the process and extracts energy from the atoms, thereby damping their motion.

Such a dissipative force can compress a beam's phase-space volume and enhance the brightness of atomic beams, enabling extraordinary sensitivity for new experiments as well as enormous improvements on old ones. We report here both experimental and theoretical studies of this new cooling process. First, we describe the active collimation of a rubidium beam in one dimension by this process, and then we present a model for it.

We use a thermal beam of natural Rb produced by an oven at $T \sim 150^\circ\text{C}$ with aperture ~ 0.33 mm diam, and a defining aperture of diam ~ 0.33 mm about 24 cm away (see Fig. 1). Both the atomic beam and the circularly polarized laser beams are horizontal, and a weak magnetic field (typically vertical) is applied perpendicular to the laser beam axis. The atomic-beam profile is measured with a vertically oriented scanning hot tungsten wire, 25 μm thick, 1.3 m away from the region of interaction with the laser beam. It ionizes virtually every Rb atom that hits it and the ion current is a measure of the beam intensity profile.

We used a Spectra-Diode Labs 2410-C laser array, injection locked to a Sharp LT021 single-stripe diode

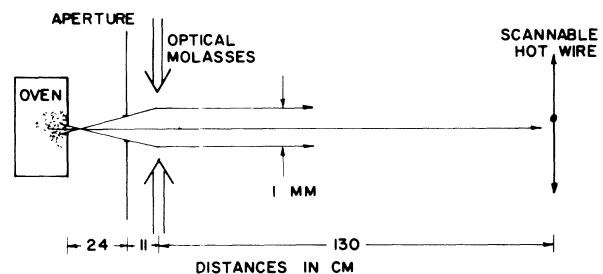


FIG. 1. Overall schematic of the apparatus used for transverse cooling.

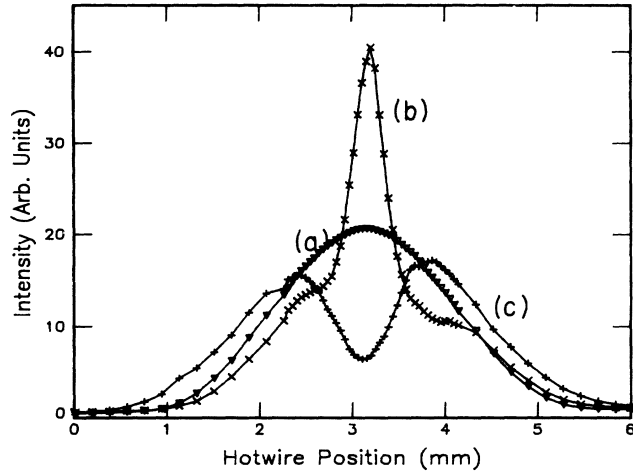


FIG. 2. Hot wire signal vs position for collimation by transverse optical molasses. For these scans, average s of the circularly polarized laser beams was $s=2.5$ and $\delta \cong \pm 3.1\gamma$. The raw data have been processed before plotting by subtracting 58% of the “no laser” signal from all three traces to correct for the presence of ^{87}Rb and ^{85}Rb ($F=2$) in the beam that is not affected by the laser light but is detected by the hot wire. The traces are laser blocked: curves a and b , $\delta < 0$, and curve c , $\delta > 0$.

laser.¹⁷ Injecting the light of the single-stripe laser collapses the full power of the array’s multimode spectral and spatial pattern into a single, diffraction-limited beam with a single-mode spectrum less than 1 MHz wide. The laser is tuned near the $F=3 \rightarrow F'=4$ transition of the $D2$ line and excited atoms necessarily decay back to $F=3$, so repumping light is not needed. The laser frequency is calibrated with a saturated absorption signal from an auxiliary Rb cell at room temperature. The laser crosses the 0.4-mm-diam atomic beam at a right angle, and is retroreflected to form the optical molasses for collimation. We use an aperture 8 mm high by 20 mm long to cut off the laser’s Gaussian tails so that the atoms traverse a $\sim 1/e^2$ change in light intensity. The total power at the interaction region is ~ 21 mW.

The efficiency of optical molasses for atomic-beam collimation is limited by the final transverse temperature achieved and the interaction time required. The characteristic damping time for the Doppler process is $\tau_c \cong 1/\gamma_c \cong 2M/\hbar k^2$ ($\sim 42 \mu\text{s}$ for Rb), where $k \cong 2\pi/\lambda$. In our 20-mm interaction region, an atom with a thermal velocity of 350 m/s spends only 60 μs , or $1.5\tau_c$, in the molasses. The damping force of magnetically induced cooling is larger (characteristic damping time τ'_c shorter), while the momentum diffusion may be comparable to that of the Doppler process. Thus the final velocity distribution is not only narrower, but approaches equilibrium faster than in the Doppler process. At the large detuning for which magnetically induced cooling is optimized, the Doppler force is very small and contributes

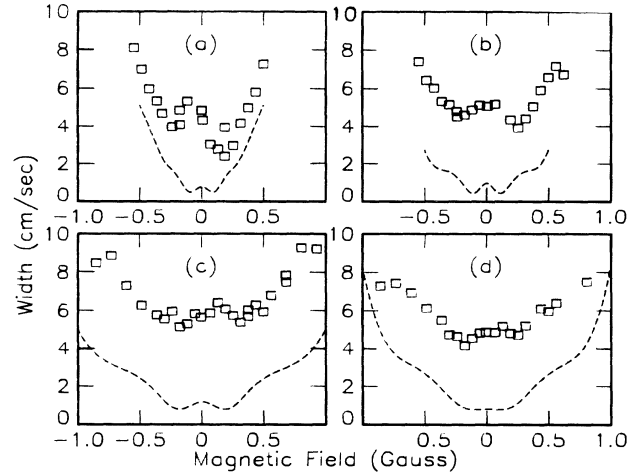


FIG. 3. Width of the velocity distribution extracted from our data vs magnetic field. (a) $s=0.8$, $\delta=-2.3\gamma$; (b) $s=2.5$, $\delta=-3.8\gamma$; (c) $s=8$, $\delta=-7.7\gamma$; and (d) $s=8$, $\delta=-10.7\gamma$. The dashed lines show the model calculations.

little to the collimation.

In Fig. 2, we show a typical measured transverse spatial distribution of the atomic beam. To extract quantitative information on the velocity distribution after collimation, we assume that the atoms captured by the cooling process leave the molasses region with a Gaussian transverse velocity distribution. We then calculate the expected beam profile at the detector and fit the parameters of this distribution to the data. Simulations show that the width of the peak of the spatial distribution becomes insensitive to the width of the velocity distribution when the latter is less than 2 cm/s (rms). This corresponds to a temperature of 4 μK . The fit to the measured profile for red tuning shown in Fig. 2 yields $v_{\text{rms}} = 3.5$ cm/s corresponding to a temperature of 12 μK or $\sim T_D/8$. In Fig. 3, we plot the final velocity spread determined from our data versus B_x for various parameters.

The cooling to sub-Doppler temperatures arises from the competition between optical pumping and Larmor precession of the ground states. To clarify the physical picture, we consider a $J=\frac{1}{2} \rightarrow \frac{3}{2}$ transition excited by σ^+ light described by an N -type transition scheme as shown in the inset of Fig. 4. We can adiabatically eliminate the excited state if the optical excitation rate is much weaker than the natural decay rate and consider the atomic behavior on a long time scale ($t \gg 1/\gamma$). This is not a real limitation, since we observe the lowest temperatures at low excitation rates. We therefore consider only two ground-state sublevels $(J, M_J) = (\frac{1}{2}, -\frac{1}{2}) \equiv |1\rangle$ and $(\frac{1}{2}, \frac{1}{2}) \equiv |2\rangle$. Atoms move along the z axis defined by the laser beam, and the magnetic field $\mathbf{B}_x = B_x \hat{x}$ is perpendicular to it. This model predicts sub-Doppler temperatures for a large range of the experi-

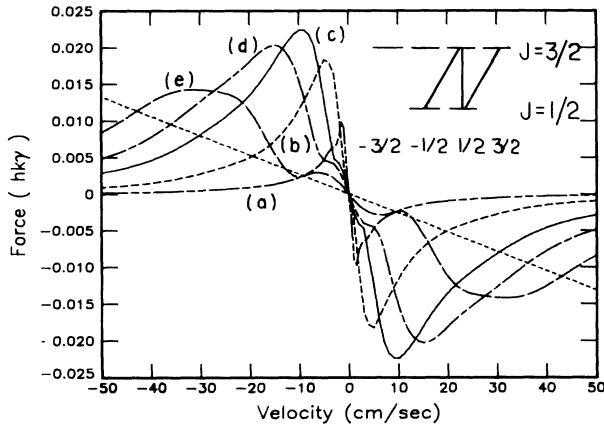


FIG. 4. Plot of the cooling force vs velocity for $s=1$ and $\delta = -1.5\gamma$. The magnetic field is, curve a, 0.01 G; curve b, 0.025 G; curve c, 0.05 G; curve d, 0.1 G; and curve e, 0.25 G. Note that the Doppler force for this intensity and detuning is much smaller than the force induced by the magnetic field and its capture range is much larger as indicated by the dashed straight line.

mental parameters.

The evolution of the reduced 2×2 ground-state density matrix is given by the Bloch equations $\dot{\rho} = [H, \rho]/i\hbar + \Gamma_{\rho}$, where the effective Hamiltonian H and the relaxation term Γ_{ρ} are written as

$$H = \hbar \begin{pmatrix} \tilde{\omega}_1 & \omega_Z \\ \omega_Z & \tilde{\omega}_2 \end{pmatrix}, \quad \Gamma_{\rho} = \begin{pmatrix} -\gamma_P \rho_{11} & -\gamma_P' \rho_{12} \\ -\gamma_P' \rho_{21} & +\gamma_P \rho_{11} \end{pmatrix}, \quad (1)$$

where $\hbar \tilde{\omega}_i = 2\hbar \delta s C_i / L$ is the light shift for the ground state $|i\rangle$. Here $\delta = \text{detuning} = \omega_{\text{laser}} - \omega_{\text{atom}}$, $L = 1 + (2\delta/\gamma)^2$, $s = \text{saturation parameter} = 2\Omega_0^2/\gamma^2$, $\Omega = \text{Rabi frequency for one beam} = \Omega_0 \cos(kz)$, and C_i is the relative transition strength. The dephasing rate γ_P' is larger than the optical pumping rate γ_P because spontaneous emission can damp the coherence between $|1\rangle$ and $|2\rangle$. From the Clebsch-Gordan coefficients we find $\gamma_P = 4\gamma s/9 \times (L + \frac{4}{3}s) \cong 4\gamma s/9L$ for $s \ll L$, and similarly $\gamma_P' = 3\gamma_P$. The Larmor-precession frequency is $\omega_Z = g_J \mu_B B_x / 2\hbar$, where $g_J = 2$ is the g factor of the ground state.

The steady-state solutions to the Bloch equations for an atom at rest give

$$\rho_{11}^s(v=0) = 1 - \rho_{22}^s(v=0) = r\omega_Z^2/D \quad (2a)$$

and

$$\rho_{12}^s(v=0) = [\rho_{21}^s(v=0)]^* = -\omega_Z(\tilde{\omega}_{12} + i\gamma_P')/D, \quad (2b)$$

where $r \equiv 2\gamma_P'/\gamma_P$, $D \equiv 2r\omega_Z^2 + \gamma_P'^2 + \tilde{\omega}_{12}^2$, and $\tilde{\omega}_{12} \equiv \tilde{\omega}_1 - \tilde{\omega}_2$. We note that in the absence of a magnetic field ($\omega_Z = 0$) all the atoms are pumped into $|2\rangle$ ($\rho_{11} = 0$) and that a very strong field equalizes the populations of $|1\rangle$ and $|2\rangle$ ($\rho_{11} = \rho_{22} = \frac{1}{2}$).

For an atom moving at velocity v we substitute $\dot{\rho} = \partial\rho/\partial t + v\nabla\rho$ in the Bloch equations and expand the elements

of ρ in a spatial Fourier series.¹⁸ For the steady-state solution, we set $\partial\rho/\partial t = 0$ and obtain recursion relations for the coefficients of the series. Truncation of the Fourier series gives us a finite set of linear equations that we solve by matrix inversion. We find good convergence when truncating after the first order at $B \sim 1$ G and after third order for smaller fields. The force on an atom is $F = -\langle \nabla H \rangle = -\text{Tr}(\rho \nabla H)$. In Fig. 4, we have plotted the average value of the force over an optical wavelength versus velocity for different values of B_x for fixed δ and s . We define $\pm v_{\text{eff}}$ as the range between the peaks of this curve. Decreasing the magnetic field increases the damping for $|v| < v_{\text{eff}}$ but decreases v_{eff} . At very small fields, only atoms with $|v| < v_{\text{eff}}$ can be effectively damped in a limited interaction time, and velocity diffusion can move them out of this narrow range. Thus the expected velocity distribution has a broad base and a small narrow peak near $v=0$.

Gordon and Ashkin¹⁹ used the quantum-regression theorem to show that the momentum diffusion of a two-level atom in a standing wave arises from the randomness of the recoil of atoms from spontaneous emission and the dipole-force fluctuations. The diffusion constant is $D_0 = (1+\alpha)\hbar^2 k^2 \gamma s / L$, where α is $\frac{2}{5}$ because of the dipole pattern.¹⁶ In our case another contribution to the diffusion constant arises from transitions between the ground-state sublevels caused by optical pumping and Larmor precession and calculate it using the method developed in Ref. 20. It applies here because the dephasing rate γ_P' is larger than the pumping rate γ_P . Therefore the Bloch equations can be well approximated by a master equation. Then

$$D_1 = [(\hbar \nabla \tilde{\omega}_{12})^2 / \gamma_P^*] \rho_{11}^s(v=0) \rho_{22}^s(v=0)$$

for this contribution, where $\gamma_P^* = \gamma_P D / (\tilde{\omega}_{12}^2 + \gamma_P'^2)$ is the pumping rate in the master equation. The total diffusion constant is just $D_0 + D_1$.

Because the force on moving atoms is not simply proportional to velocity, we calculate the velocity distribution from the steady-state solution of the Fokker-Planck equation,²¹ using our numerical results for force and the diffusion constant. We then determine the rms width of this distribution, v_{rms} , and associate it with the final temperature, $k_B T = M v_{\text{rms}}^2$. This procedure makes it impossible to give an analytical expression for the final temperature of this cooling process. However, from our numerical results we can extract the following scaling properties for the temperature. For fixed detuning and B , the temperature increases for both small and large intensities. If B is scaled proportional to s , then the final temperature decreases with s for $s < L$ as in other cases.^{6,13,14} We find that v_{eff} is almost linear in B and independent of s , so that decreasing s and B together reduces v_{eff} to the order of v_{rms} , thereby increasing the temperature, thus providing its lower limit. We have obtained temperatures as low as $5 \mu\text{K}$ in our model.

To compare the results from the model with the data,

we have extended our calculation for the damping force to include all seven sublevels of the $F=3$ ground state of Rb, and expanded all 49 density matrix elements in Fourier series. Solving the resulting system of linear equations yields the force on the atoms, which turns out larger than for the two-level model. From these calculations we also find that the damping time τ'_c is much smaller than τ_c , and this is supported by our measurements showing that over a large range of parameters, shortening the interaction region length by 25% has little effect on the measured distribution width.

Generalizing the diffusion to include all the substates is a much more difficult problem. As an estimate, we have used the diffusion calculated from our $\frac{1}{2} \rightarrow \frac{3}{2}$ model to determine the width of the narrow peak of the velocity distribution for comparison with our data. We have plotted this calculated width as the dashed lines in Fig. 3. The difference between the actual and estimated diffusion is most likely responsible for the discrepancies.

Increasing the field beyond the maximum value used in Fig. 4 changes the sign of the slope of the force in the vicinity of $v=0$. This suggests that atoms can be cooled instead of heated when $\delta > 0$, and we have observed this effect with a magnetic field of a few gauss. This occurs at both low and high intensities, if the magnetic field is increased proportionally to the intensity. It is important to emphasize that this is *not* the same as the stimulated emission cooling.²² This topic is under active study.

An atom moving along the standing wave is subject to the conservative force from an array of potential wells with a period of $\lambda/2$. The depth of each well is equal to the ac Stark shift at the antinodes and is comparable to the kinetic energy of atoms that are captured by the cooling mechanism. Atoms may therefore be confined between planes formed by the standing wave's nodes. We are presently studying this channeling for a future publication.

We acknowledge much helpful discussion with Tom Bergeman. This work was supported by the NSF and the ONR.

^(a)Present address: Physics Department, Caltech, Pasadena, CA 91125.

¹T. Hansch and A. Schawlow, *Opt. Commun.* **13**, 68 (1975).

²D. Wineland and H. Dehmelt, *Bull. Am. Phys. Soc.* **20**, 637 (1975).

³S. Stenholm, *Rev. Mod. Phys.* **58**, 699 (1985). This paper contains a review of early theoretical works and many references.

⁴V. Balykin *et al.*, *Pis'ma Zh. Eksp. Teor. Fiz.* **40**, 251 (1984) [*JETP Lett.* **40**, 1026 (1984)].

⁵S. Chu *et al.*, *Phys. Rev. Lett.* **55**, 48 (1985).

⁶J. Dalibard *et al.*, in *Proceedings of the Eleventh International Conference on Atomic Physics, Paris, France, 1988*, edited by S. Haroche, J. C. Gay, and G. Grynberg (World Scientific, Singapore, 1989), p. 199.

⁷A. Aspect *et al.*, *Phys. Rev. Lett.* **61**, 826 (1988).

⁸D. Sesko *et al.*, *J. Opt. Soc. Am. B* **4**, 1225 (1988).

⁹P. Lett *et al.*, *Phys. Rev. Lett.* **61**, 169 (1988).

¹⁰Y. Shevy *et al.*, *Phys. Rev. Lett.* **62**, 1118 (1989).

¹¹P. Lett *et al.*, *J. Opt. Soc. Am. B* **6**, 2084 (1989).

¹²D. Wineland and W. Itano, *Phys. Rev. A* **20**, 1521 (1979).

¹³J. Dalibard and C. Cohen-Tannoudji, *J. Opt. Soc. Am. B* **6**, 2023 (1989).

¹⁴S. Chu *et al.*, in *Proceedings of the Eleventh International Conference on Atomic Physics, Paris, France, 1988* (Ref. 6), p. 636.

¹⁵This method was suggested by J. Dalibard *et al.*, in *Proceedings of the Eleventh International Conference on Atomic Physics, Paris, France, 1988* (Ref. 6). After completion of this paper, two relevant papers appeared; see P. Ungar *et al.*, *J. Opt. Soc. Am. B* **6**, 2058, (1989), and D. Weiss *et al.*, *ibid.* **6**, 2072 (1989).

¹⁶J. Javanainen and S. Stenholm, *Appl. Phys.* **21**, 35 (1980).

¹⁷S.-Q. Shang and H. Metcalf, *Appl. Opt.* **28**, 1618 (1989).

¹⁸V. Minogin and O. Serimaa, *Opt. Commun.* **30**, 373 (1979).

¹⁹J. Gordon and A. Ashkin, *Phys. Rev. A* **21**, 1606 (1980).

²⁰J. Dalibard and C. Cohen-Tannoudji, *J. Opt. Soc. Am. B* **2**, 1707 (1985).

²¹H. Risken, *The Fokker-Planck Equation, Methods of Solution and Applications* (Springer-Verlag, Berlin, 1984), p. 96.

²²A. Aspect *et al.*, *Phys. Rev. Lett.* **57**, 1688 (1986).